JOURNAL OF SOLID STATE CHEMISTRY **121,** 158–166 (1996)
ARTICLE NO. 0023

Magnetic Properties of the Oxygen Deficient Perovskites $La_{0.5}Ba_{0.5}Co_{1-x}Fe_xO_{3-\delta}$

Y. Minet, V. Lefranc, N. Nguyen,[1] B. Domengès, A. Maignan, and B. Raveau

Laboratoire CRISMAT, URA1318 associée au CNRS, ISMRA et Université de Caen, Bd du Maréchal Juin, 14050 Caen Cedex, France

Received May 22, 1995; in revised form September 1, 1995; accepted September 13, 1995

New perovskites characterized by a complex mixed valence of transition elements have been isolated: $La_{0.5}Ba_{0.5}Co_{1-x}Fe_xO_{3-\delta}$ ($0 \le x \le 1$ and $0.05 \le \delta \le 0.07$) with the cubic symmetry, and $La_{0.5}Ba_{0.5}Co_{0.5}Fe_{0.5}O_{2.65}$ with the tetragonal symmetry ($a \approx a_p$, $c \approx 2a_p$). The structure of the latter has been described as $YBaFeCuO_5$-type 90° oriented domains distributed in a stoichiometric perovskite matrix $La_{0.5}Ba_{0.5}Co_{0.5}Fe_{0.5}O_3$. The Mössbauer study of these phases has allowed the two species Fe(III) and Fe(IV) to be evidenced: no proof of disproportionation of Fe(IV) into Fe(III) and Fe(V) has been obtained. The cobalt mixed valence Co(III)–Co(IV) has been deduced from the Mössbauer study coupled with the chemical analysis for the oxidized samples $La_{0.5}Ba_{0.5}Co_{1-x}Fe_xO_{3-\delta}$, whereas the reduced phase $La_{0.5}Ba_{0.5}Co_{0.5}Fe_{0.5}O_{2.65}$ is characterized by the mixed valence Co(II)–Co(III). The magnetic susceptibility measurements of $La_{0.5}Ba_{0.5}Co_{1-x}Fe_xO_{3-\delta}$ show an evolution from an antiferromagnetic behavior for $x \ge 0.50$ with T_N ranging from 142 to 218 K, to a ferromagnetic behavior for $x < 0.50$ with T_c ranging from 120 to 150 K. The tetragonal phase $La_{0.5}Ba_{0.5}Co_{0.5}Fe_{0.5}O_{2.65}$ is antiferromagnetic with $T_N \approx 480$ K. All the antiferromagnetic phases exhibit a second transition at $T_B < T_N$. The origin of the latter is not explained for the cubic phases and may correspond to a change of spin orientation of the transition element species in the case of the tetragonal phase. © 1996 Academic Press, Inc.

INTRODUCTION

Perovskite-type oxides of the transition elements of the first period have attracted considerable interest these past eight years because of their unexpected magnetic and transport properties. This is the case of the mixed valent copper oxides studied for their superconducting properties at high temperature and for the mixed valent manganese perovskites that exhibit giant magnetoresistance effects. Although extensively studied, the origin of these properties, that deals with relationships between electronic transport properties and magnetism, is so far not understood. In this respect, mixed valent iron and cobalt oxides should be also of great interest, since these elements may also exhibit two or even more electron configurations for the same oxidation state.

The consideration of the mixed valent iron and cobalt perovskites $La_{1-x}A_xMO_{3-y}$ (M = Fe or Co) shows two different behaviors. In $La_{1-x}A_xFeO_{3-y}$ (1–5) with A = Sr, Ba antiferromagnetic properties are obtained which are correlated with a disproportionation of Fe(IV) into Fe(V) and Fe(III). The cobalt perovskite $La_{1-x}Sr_xCoO_3$ has been studied by various techniques (6–10). One observes a spin glass behavior for low x values, that ascribed to the frustration of random competing interactions which are ferromagnetic between Co(III) and Co(IV) and antiferromagnetic between identical species (Co(III)–Co(III) or Co(IV)–Co(IV)) (9). In this system the spin changes with x, so that for $0 \le x \le 0.50$, Co(III) is in the low-spin state with (t_{2g}^6) and Co(IV) is in the high-spin state with ($t_{2g}^3 e_g^2$) (9), whereas for $x > 0.5$ the reverse is observed, i.e., high-spin Co(III) and low-spin Co(IV) (10). For the barium cobalt perovskites, two compositions, $La_{0.33}Ba_{0.66}CoO_{2.33+y}$ and $La_{0.5}Ba_{0.5}CoO_3$, have been isolated (11, 12), but the physical properties of the latter phase are not yet studied and the valence state of Co is not specified for the former.

The consideration of all these results suggests that the study of perovskites in the system La–Ba–Co–Fe–O should be of great interest. The present paper deals with the crystallographic, magnetic, and Mössbauer studies of new perovskites $La_{0.5}Ba_{0.5}Co_{1-x}Fe_xO_{3-\delta}$, with x ranging from 0 to 1.

EXPERIMENTAL

Polycrystalline samples of nearly stoichiometric perovskites $La_{0.5}Ba_{0.5}Co_{1-x}Fe_xO_{3-\delta}$ (with $\delta \approx 0$) were prepared by solid state reaction of La_2O_3, $BaCO_3$, Fe_2O_3, and Co_3O_4 mixed in the stoichiometric molar proportions and initially decarbonated at 950°C for 24 hr in air. After regrinding, the samples were heated for 2 days at 1200°C and slowly furnace cooled. Note that for the $x = 1$ composition, a full reaction was obtained by repeating this process three times.

[1] To whom correspondence should be addressed.

0022-4596/96 $12.00

In an attempt to synthesize oxygen deficient perovskites, $La_{0.5}Ba_{0.5}Co_{1-x}Fe_xO_{3-\delta}$ were prepared by a two step procedure. First, the appropriate mixtures of La_2O_3, $BaCO_3$, and Fe_2O_3 were heated at 950°C for 24 hr in air. Second, adequate amounts of Co_3O_4, Co, and/or Fe were added in order to reach the oxygen content $O_{3-\delta}$, the final mixtures were heated in an evacuated silica ampoule for 3 days at 900°C, and finally were slowly cooled to room temperature.

The purity of the phases was confirmed by X-ray diffraction by means of a Philips diffractometer using Cu$K\alpha$ radiation. Powder X-ray diffraction data were collected at 293 K by step scanning over an angular range from 6° to 90° in 2 θ with an increment of 0.02°. Lattice constants were refined and structural calculations were performed using the profile analysis program DBW 3.2 (13).

Electron diffraction was carried out on a JEM 200CX equipped with a (±60°) tilting-rotating goniometer, and high resolution was performed on a TOPCON 2B microscope equipped with ±10° double tilt goniometer and objective lens with Cs = 0.4 mm.

The oxygen content was determined by chemical analysis using a redox back titration method. Fe^{4+}, Fe^{3+}, Co^{3+}, Co^{4+},... species, if they exist, were reduced into Fe^{3+} and Co^{2+} by a known amount of Fe^{2+} chloride in acid solution. The amount of unreacted Fe^{2+} was then determined by titration with potassium dichromate.

Magnetic susceptibility measurements were carried out from 4 to 850 K using the Faraday balance or a S.Q.U.I.D. magnetometer for the cobalt rich compounds. Hysteresis loops were registered at 4 K in a FONER vibrating sample magnetometer.

Mössbauer powder absorption spectra of ^{57}Fe were obtained in a transmission geometry with a constant acceleration spectrometer using a ^{57}Co source in a Rh matrix. Spectra were fitted using the MOSFIT program (14). The powder samples enriched with 2% ^{57}Fe were studied at 4.2 and 293 K. The isomer shift values are given with respect to metallic iron.

Resistive measurements were carried out by using a four-probe method in the range $10 \leq T \leq 293$ K.

RESULTS AND DISCUSSION

Structural Characterization

The air synthesized phases $La_{0.5}Ba_{0.5}Co_{1-x}Fe_xO_{3-\delta}$ exhibit a cubic symmetry whatever x, ranging from 0 to 1. The oxygen deficiency is small ($0.05 \leq \delta \leq 0.07$). The lattice parameter of these perovskites increases as x increases (Fig. 1) in agreement with the larger size of iron compared to that of cobalt.

In reducing conditions, only one phase corresponding to the composition $La_{0.5}Ba_{0.5}Fe_{0.5}Co_{0.5}O_{2.65}$ could be isolated as a pure sample. The X-ray diffraction pattern can

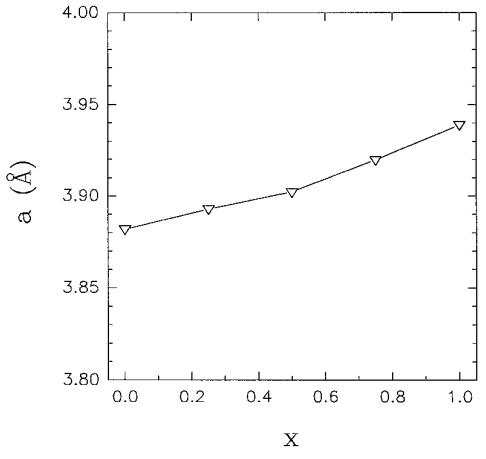

FIG. 1. Evolution of the cubic cell parameter vs x composition for the $La_{0.5}Ba_{0.5}Co_{1-x}Fe_xO_{3-\delta}$ phases.

be indexed in the tetragonal cell with $a = 3.966$ (1) Å $\approx a_p$, $c = 7.777$ (1) Å $\approx 2a_p$. Nevertheless, the electron diffraction (ED) investigation of this sample shows that the true symmetry of most microcrystals is not tetragonal but orthorhombic. Indeed, besides a strong "$a_p \times a_p \times 2a_p$" subcell, weak extra dots on ED patterns reveal a doubling of one parameter in the (a–b) plane (Fig. 2a) leading to a "$a \times 2a_p \times c$" ($a \approx a_p$, $c \approx 2a_p$) orthorhombic

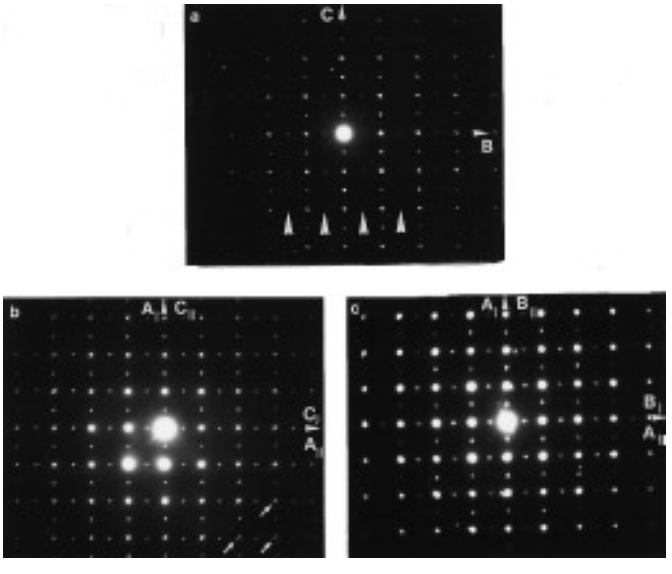

FIG. 2. Three examples of electron diffraction patterns of $La_{0.5}Ba_{0.5}Co_{0.5}Fe_{0.5}O_{2.65}$ microcrystals. (a) [100], very weak extra dots (arrowed) double the b parameter. (b) [010], two 90° oriented (a, c) domains. Note the splitting of dots (small arrows) due to the ratio $2a/c = 1.02$, parallel to [102]*, indicates a twinning phenomenon with twinning boundary parallel to [102] plane (i.e., [101] plane of the perovskite subcell). (c) [001], two 90° oriented (a, b) domains. Extra dots doubling the b parameter are quite strong.

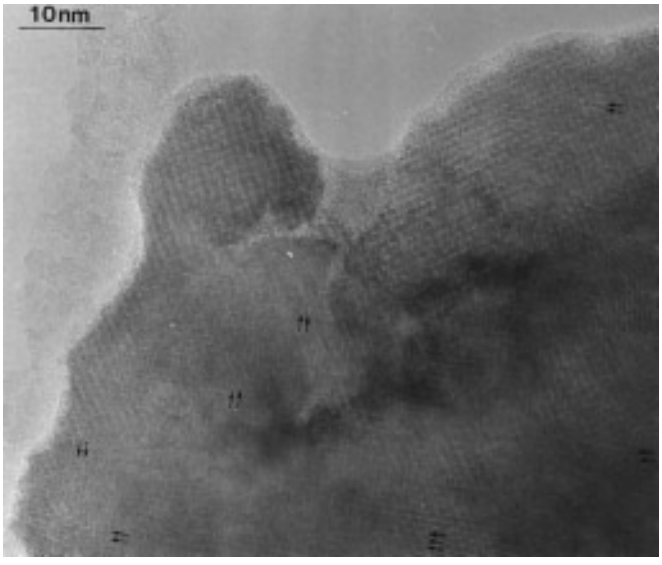

FIG. 3. Medium magnification high resolution image corresponding to Fig. 2c ED pattern. Modulation of contrast following the $2 \times a_p$ periodicity (small arrows) is observed along both *a* and *b* directions on very local domains spread over the matrix.

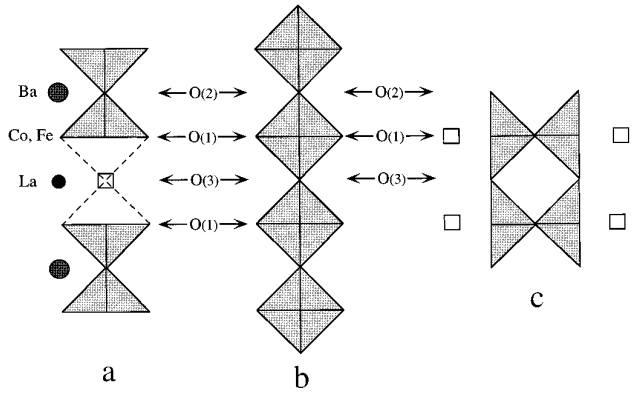

FIG. 4. Scheme showing the two $YBaFeCuO_5$-type 90° oriented domains ((a) and (c)) distributed in a stoichiometric perovskite matrix (b).

cell. Another phenomenon evidenced by electron diffraction is the frequent observation of 90° oriented domains (Figs. 2b and 2c). This may concern the [010] plane as well as the [001] plane. This phenomenon, which was similarly observed in La–Ba–Cu 123-type oxides (15), is related to the La–Ba similar sizes and ability to occupy the same sites so that the La–Ba ordering may take place in the three crystallographic ⟨100⟩ axes of the perovskite, forming nanodomains. Thus, direct observations by high resolution electron microscopy of the doubling of one parameter in the (*a*–*b*) plane show local variations of the contrast following the 2*a* periodicity along both *a*, *b* directions (Fig. 3). This may be related to an ordering of the oxygen vacancies but localized on very tiny domains. Thus, the resulting X-ray diffraction pattern, characteristic of a mean structure, does not show any extra reflections and structure calculations were performed in the most symmetrical space group *P*4/*mmm* in the "$a_p \times a_p \times 2a_p$" cell.

Considering the results previously obtained for the oxygen deficient perovskites $Y_{0.5}Ba_{0.5}(Co, Cu, Fe)_1O_{2.5}$ (16–19) that exhibit the $YBaFeCuO_5$ structure (17) which is built up from double pyramidal layers interleaved with Y ions, the La^{3+}, Ba^{2+}, and $(Co, Fe)^{n+}$ ions were located in the Y, Ba, and (Cu, Fe) sites of this structure, respectively (Fig. 4a). Although, in a first step the apical O(2) site and the equatorial O(1) site were considered as fully occupied. The 0.30 excess oxygen with respect to the O_5 formulation was statistically distributed over the O(3) site, corresponding to the second apical site forming the $(Co, Fe)O_6$ octahedra (Fig. 4b) in the stoichiometric perovskite.

The refinements of the variable atomic coordinates and thermal factors lead to a reliability factor *Ri* calculated on the intensities of 0.06. Then, the refinement of the oxygen occupation in the different sites, O(1), O(2), and O(3), allowed the reliability factor to be lowered to $Ri = 0.04$ for a partial occupancy of the O(1) site (10% vacancy) and of the O(3) site (30% vacancy), the O(2) site being fully occupied. The final variable parameters are listed in Table 1; A good fit is obtained between the observed and calculated XRD patterns (Fig. 5). The corresponding bond lengths (Table 2) show that the (Co, Fe)–O distances are generally larger than those obtained for the air-synthesized phase $La_{0.5}Ba_{0.5}Co_{0.5}Fe_{0.5}O_{2.95}$ (= 1.951 Å); this agrees with the smaller oxidation state of the transition elements for this reduced tetragonal perovskite. Thus, in agreement with electron microscopy observations the structure of these tetragonal crystals can be described as the coexistence of tiny microdomains of composition $LaBa(Co, Fe)_2O_5$ with the $YBaFeCuO_5$ structure 90° oriented with respect to each other (Figs. 4a–4c) dispersed in a matrix of the stoichiometric perovskite $LaBaCoFeO_6$ (Fig. 4b). The coexistence of such microdomains is made possible because the apical (Co, Fe)–O bond of the pyramid is

TABLE 1
Refined Atomic Parameters for the Tetragonal $La_{0.5}Ba_{0.5}Co_{0.5}Fe_{0.5}O_{2.65}$ Phase[a]

Atom	Site	*x*	*y*	*z*	*B* (Å)^2	Occ
La	1b	0	0	0.5	1.0 (1)	1
Ba	1a	0	0	0	0.4 (1)	1
(Co, Fe)	2h	0.5	0.5	0.25	0.1 (1)	2
$O_{(1)}$	4i	0.5	0	0.2788(2)	1.0	3.6
$O_{(2)}$	1c	0.5	0.5	0	1.0	1
$O_{(3)}$	1d	0.5	0.5	0.5	1.0	0.7

[a] Space group *P*4/*mmm*, $Z = 2$, $a = b = 3.9659$ (3) Å, $c = 7.7773$ (7) Å.

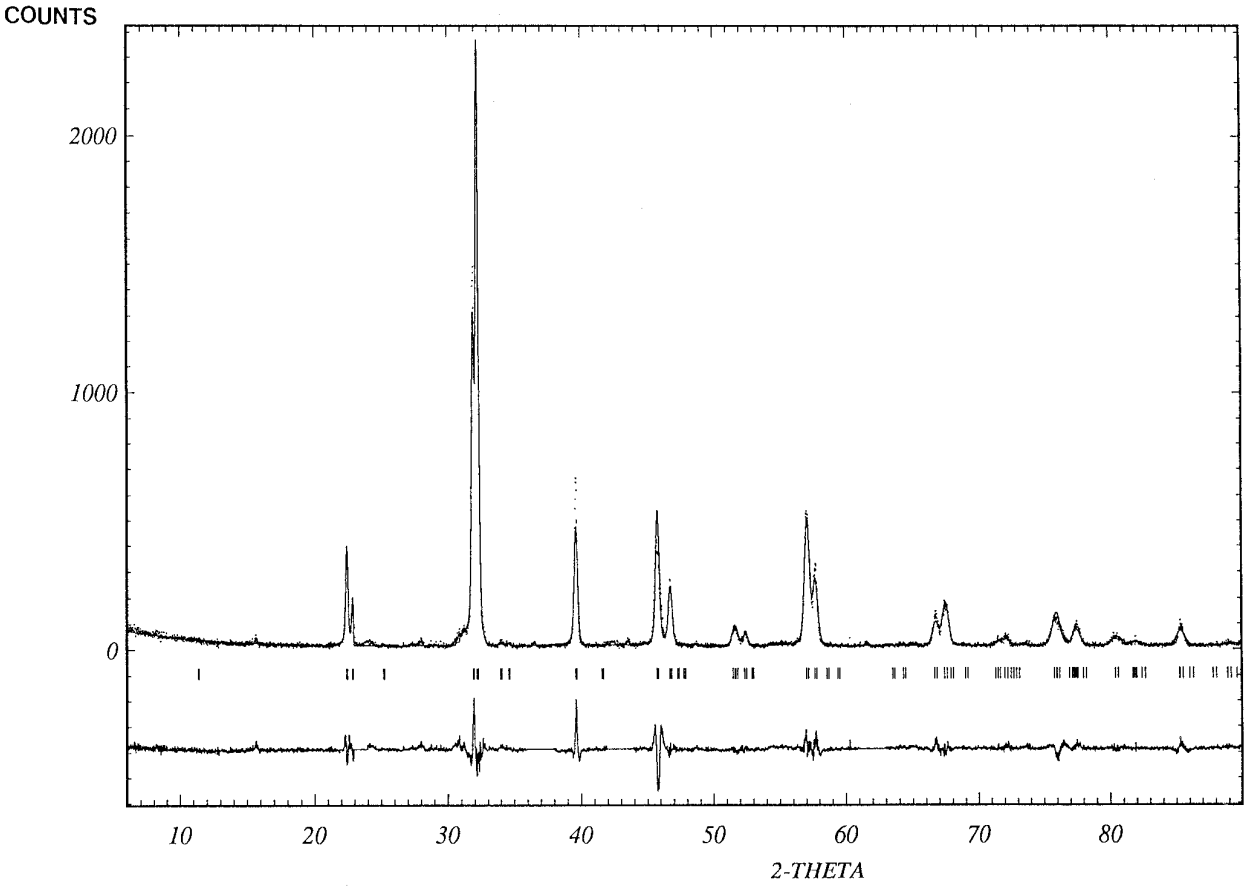

FIG. 5. Observed, calculated, and difference X-ray powder diffractogram of the $La_{0.5}Ba_{0.5}Co_{0.5}Fe_{0.5}O_{2.65}$.

rather close to the equatorial bonds, avoiding a dramatic anisotropy, in contrast to the cuprates for which the Jahn–Teller effect is strongly pronounced.

Mössbauer Spectroscopy

Cubic perovskites $La_{0.5}Ba_{0.5}Co_{1-x}Fe_xO_{3-\delta}$. The oxygen content determined by chemical analysis suggests that various oxidation states are possible for the involved elements such as Fe(III, Fe(IV), Fe(V), Co(III), and Co(IV). In order to determine the nature of the different species, a Mössbauer investigation of $La_{0.5}Ba_{0.5}Co_{1-x}Fe_xO_{3-\delta}$ ($0.25 \leq x \leq 1$) has been performed, allowing the valence state of cobalt to be deduced from this study.

TABLE 2
Bond Lengths for the $La_{0.5}Ba_{0.5}Co_{0.5}Fe_{0.5}O_{2.65}$ Phase

	d (Å)
$La–O_{(3)}$	2.804×4
$La–O_{(1)}$	2.625×8
$Ba–O_{(2)}$	2.804×4
$Ba–O_{(1)}$	2.938×8
$Co/Fe–O_{(1)}$	1.995×4
$Co/Fe–O_{(2)}$	1.944×1
$Co/Fe–O_{(3)}$	1.944×1

Mössbauer spectra of the air-synthesized phases were performed at 4 and 293 K (Figs. 6 and 7). The room temperature spectra indicate the presence of pure electric quadrupolar interactions. They can be analyzed as two and three quadrupole components for $x \leq 0.5$ and $x > 0.5$, respectively (Table 3). At 4 K, all the spectra show a magnetic ordering (Fig. 6) consistent with the behavior observed at low temperature by the magnetic susceptibility measurements that will be presented further. These have been easily fitted by the presence of two main magnetic sites, labeled A and B. Except for $La_{0.5}Ba_{0.5}FeO_{2.93}$, the large asymmetry of the outer-lines of the A sextet imposes the introduction of a second sextet (H_f = 53.2 T) to obtain a correct fit (Table 3). Note that all the sextets have broadened lines and very small or negligible quadrupole shift (2ε) values. The minor paramagnetic C contribution ob-

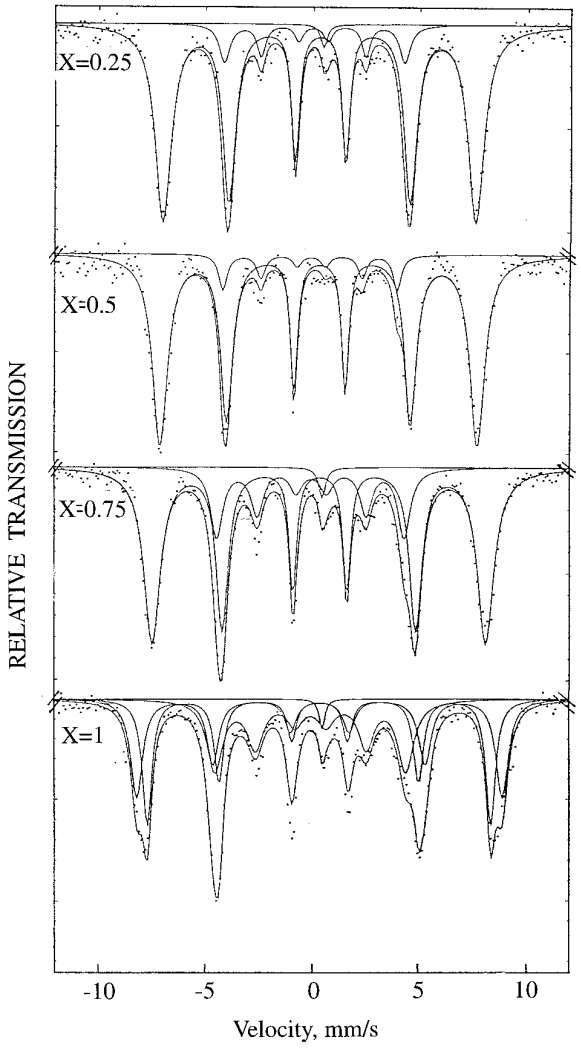

FIG. 6. The Mössbauer spectra at 4.2 K of $La_{0.5}Ba_{0.5}Co_{1-x}Fe_xO_{3-\delta}$ cubic oxides.

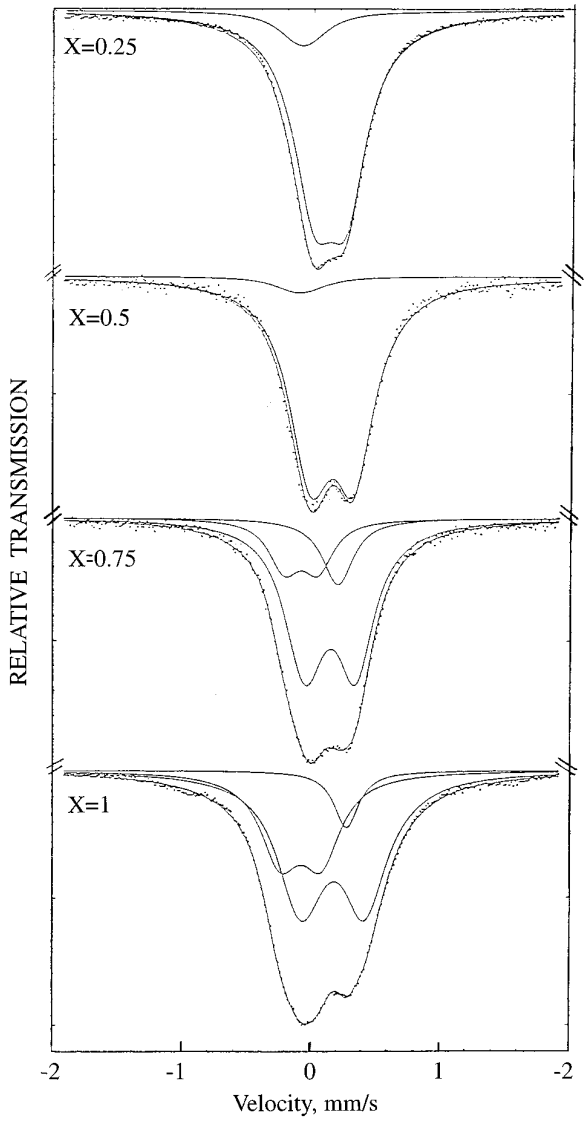

FIG. 7. The Mössbauer spectra at room temperature of $La_{0.5}Ba_{0.5}Co_{1-x}Fe_xO_{3-\delta}$ cubic oxides.

served on some of spectra at 4 and 293 K with $\Delta E_q = 0$ can be considered as a trivalent iron oxide, impurity not identified in our phases by X-ray diffraction.

The isomer shift (IS) and hyperfine field (H_f) values observed at 4 or 293 K of the A sites are typical of trivalent iron. On the other hand, the interpretation of the B sites is more ambiguous because their IS (0.02–0.13 mm/sec) and H_f values (26.2–27.3 T) are in the range which is not only found for Fe(IV) (20) but also for Fe(V) (1, 4).

At this stage, it is necessary to take into account the previous Mössbauer results obtained by Gibb and Matsuo (1) for $La_{0.5}Ba_{0.5}FeO_{2.97}$, which are also reported in Table 3. The values of IS and H_f obtained by these authors are close to those observed here for $La_{0.5}Ba_{0.5}Co_{1-x}Fe_xO_{3-\delta}$, but beside the B site, only one magnetic A site has been identified for Fe(III) on their spectrum at 4 K. These authors have interpreted their Mössbauer results at 4 K and room temperature in terms of a nominal charge disproportionation $2Fe(IV) \rightleftarrows Fe(III) + Fe(V)$ with decreasing temperature which is related to the onset of the magnetic ordering. They have established this process from the comparison of the oxygen content deduced by Mössbauer study with that observed by chemical analysis ($O_{2.97}$). An agreement is found between the results obtained by these two methods when they attribute the B site to Fe(V) at 4 K and to Fe(IV) at 293 K. The computed ratio of $[B]_{293\,K} = [Fe^{4+}]_{293\,K} = 38\%$ is two times higher than that of $[B]_{4\,K} = [Fe^{5+}]_{4\,K} = 22\%$. This supports the charge disproportionation hypothesis. Moreover, the isomer shift

TABLE 3
Fitted Hyperfine Mössbauer Parameters at 4.2 and 293 K of $La_{0.5}Ba_{0.5}Co_{1-x}Fe_xO_{3-\delta}$ Phases

	4.2 K					293 K		
Cubic phases	IS ± 0.02 (mm/sec)	2ε ± 0.02 (mm/sec)	H_f ± 0.1 (T)	% ± 5	Site	IS ± 0.02 (mm/sec)	ΔE_q ± 0.02 (mm/sec)	% ± 5
$x = 0.25$	0.41	−0.03	45.5	87	A	0.24	0.25	90
$\delta = 0.05$	0.13	0.10	26.2	12	B	0.03	0.08	10
	0.56	0.0	—	1	C			
$x = 0.5$	0.41	−0.02	48.3	91	A	0.27	0.34	93
$\delta = 0.05$	0.02	−0.02	26.5	9	B	0.01	0.11	7
$x = 0.75$	0.44	−0.03	48.6	76	A	0.26	0.40	70
$\delta = 0.05$	0.06	−0.01	27.3	22	B	0.03	0.26	19
	0.56	0.0	—	2	C	0.32	0.0	11
$x = 1$	0.46	−0.01	53.2	32	A	0.29	0.50	60
$\delta = 0.07$	0.45	−0.02	50.1	34				
	0.06	0.03	27.8	32	B	0.04	0.32	33
	0.58	0.00	—	2	C	0.39	0.0	7
Ref. (4)	0.43	—	51.0	78	A	0.28	0.39	62
$x = 1$	0.01	—	27.1	22	B	0.10	0.35	38
$\delta = 0.03$								
					IS	2ε	H_f	%
Tetragonal phase	0.44	0.30	54.3	18	0.39	0.35	48.7	17
$x = 0.5$	0.43	−0.24	51.9	82	0.33	−0.27	44.3	83
$\delta = 0.35$								

value of the B site at 293 K is abnormally higher than that at low temperature. Indicative of an effective change in oxidation state of this site.

In $La_{0.5}Ba_{0.5}Co_{1-x}Fe_xO_{3-\delta}$, the [B] ratio is nearly unchanged with temperature effect (Table 3) whatever x may be, and its isomer shift decreases with increasing temperature. This suggests that at low or high temperature, this site keeps the same nature. Thus, the charge disproportionation can be ruled out for $La_{0.5}Ba_{0.5}Co_{1-x}Fe_xO_{3-\delta}$. For our $La_{0.5}Ba_{0.5}FeO_{2.93}$ iron compound, the [B] ratio = 33% and the oxygen content value (2.93) lead us to attribute the B component to the presence of Fe(IV). In the other compounds of the $La_{0.5}Ba_{0.5}Co_{1-x}Fe_xO_{3-\delta}$ solid solution, the IS and H_f values are not much different (Table 3) from those of $La_{0.5}Ba_{0.5}FeO_{2.93}$, and the [B] amount increases with x.

TABLE 4
Detailed Formulas of the $La_{0.5}Ba_{0.5}Co_{1-x}Fe_xO_{3-\delta}$ Oxides

$x = 0$	$La_{0.5}Ba_{0.5}Co^{III}_{0.6}Co^{IV}_{0.4}O_{2.95}$
$x = 0.25$	$La_{0.5}Ba_{0.5}Co^{III}_{0.375}Co^{IV}_{0.375}Fe^{III}_{0.225}Fe^{IV}_{0.025}O_{2.95}$
$x = 0.5$	$La_{0.5}Ba_{0.5}Co^{III}_{0.15}Co^{IV}_{0.35}Fe^{III}_{0.45}Fe^{IV}_{0.05}O_{2.95}$
$x = 0.75$	$La_{0.5}Ba_{0.5}Co^{III}_{0.0}Co^{IV}_{0.25}Fe^{III}_{0.60}Fe^{IV}_{0.15}O_{2.95}$
$x = 1$	$La_{0.5}Ba_{0.5}Fe^{III}_{0.64}Fe^{IV}_{0.36}O_{2.93}$

Thus, it can be asserted that in all the cubic perovskites $La_{0.5}Ba_{0.5}Co_{1-x}Fe_xO_{3-\delta}$, the B site is occupied by Fe(IV). This allows a detailed formulation of those phases (Table 4) to be proposed. The examination of the latter shows that Co(IV) species are more easily found than Fe(IV), in agreement with the $3d^5$ electronic configuration of Co(IV) which is isoelectronic to Fe(III).

The tetragonal perovskite $La_{0.5}Ba_{0.5}Co_{0.5}Fe_{0.5}O_{2.65}$. The Mössbauer patterns of this phase, registered at 4.2 and 293 K, evidence the magnetic character of iron species even at room temperature (Figs. 8a and 8b), showing two magnetic hyperfine areas in the ratio of about 18/82 (Table 3). The isomer shift and the hyperfine field values of both sites at 4.2 and 293 K are typical of Fe(III) ($S = 5/2$). However, the signs of the quadrupole shift 2ε are opposed. This means that the environment symmetry of these two Fe(III) sites is different. This is probably due to the presence of oxygen vacancies. Nevertheless, the second Mössbauer site corresponding to about 80% of intensity can be attributed to the pyramidal environment of iron on account of its lower values of H_f and IS with respect to those observed for the first site.

According to the oxygen amount $O_{2.65}$ and the Mössbauer results, the chemical formula of this tetragonal phase can be written as $La_{0.5}Ba_{0.5}Co^{II}_{0.2}Co^{III}_{0.3}Fe^{III}_{0.5}O_{2.65}$.

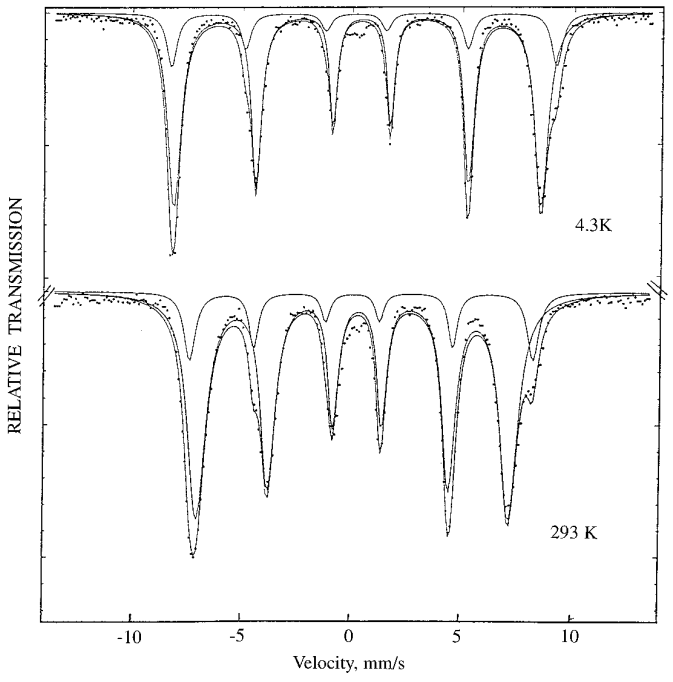

FIG. 8. Mössbauer powder spectra of $La_{0.5}Ba_{0.5}Co_{0.5}Fe_{0.5}O_{2.65}$ tetragonal phase at 4.3 K and room temperature.

Magnetic Susceptibility Study

The thermal evolutions of the inverse magnetic molar susceptibility χ_M^{-1} of the cubic phases $La_{0.5}Ba_{0.5}Co_{1-x}Fe_xO_{3-\delta}$ are shown in Fig. 9. They show an evolution of the magnetic property from antiferromagnetic behavior for $x \geq 0.5$ to ferromagnetic behavior for $x < 0.5$ as the iron content decreases.

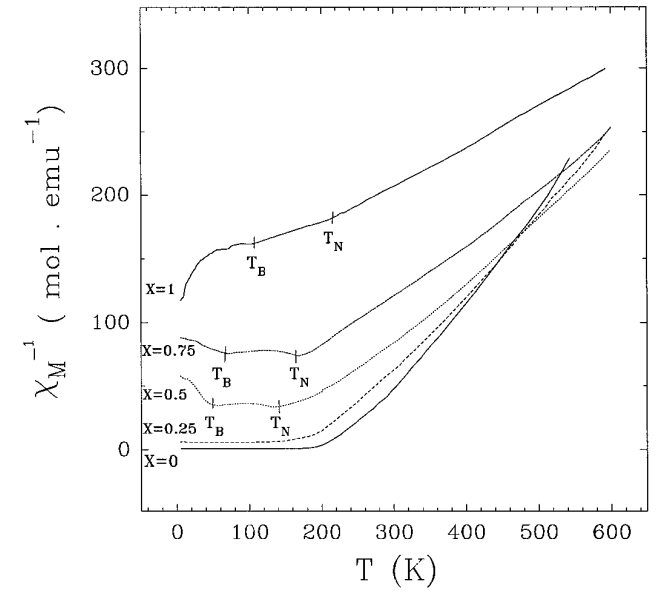

FIG. 9. Reciprocal molar magnetic susceptibility vs temperature of $La_{0.5}Ba_{0.5}Co_{1-x}Fe_xO_{3-\delta}$ cubic phases.

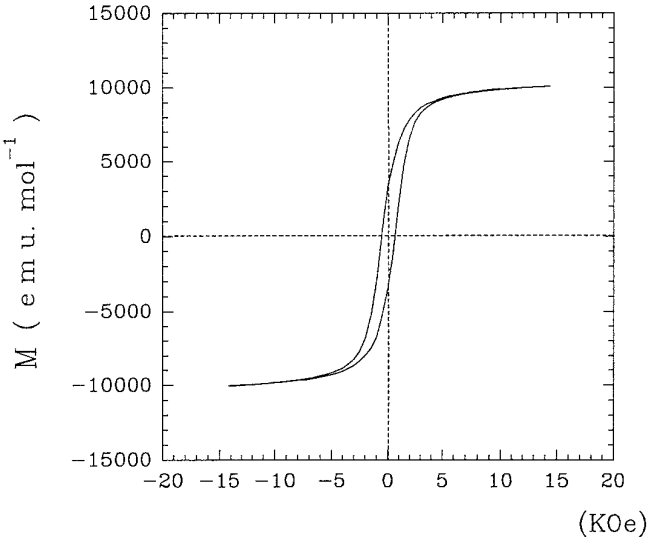

FIG. 10. Magnetization of $La_{0.5}Ba_{0.5}CoO_{2.95}$ ($x = 0$) as a function of applied field at 4.2 K.

For the ferromagnetic compounds, M at 4.2 K does not reach its saturation value in the applied magnetic field of 15 kOe (Fig. 10). The corresponding measured magnetic moment per mole is equal to 1.28 and 1.83 μ_B for $x = 0.25$ and $x = 0$ compounds, respectively, in agreement with the value of 1.9 μ_B observed for $La_{0.5}Sr_{0.5}CoO_3$ (9). The magnetization curve of $La_{0.5}Ba_{0.5}CoO_{3-\delta}$ versus temperature (Fig. 11) shows that the T_c (Curie temperature) is

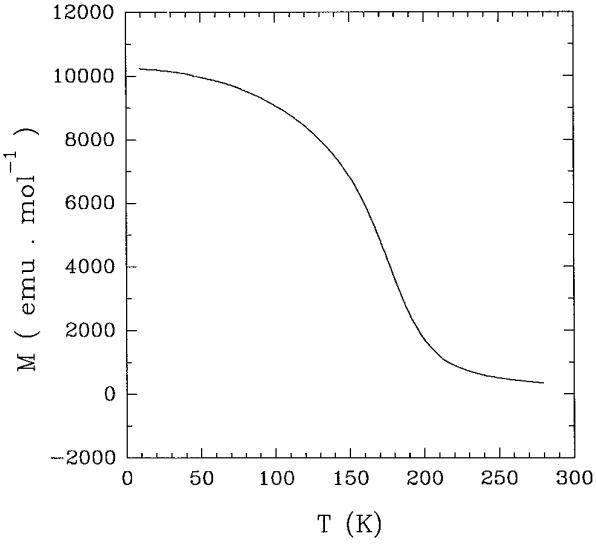

FIG. 11. Magnetization vs temperature of $La_{0.5}Ba_{0.5}CoO_{2.95}$ measured in the magnetic field of 15 kOe after zero field cooling.

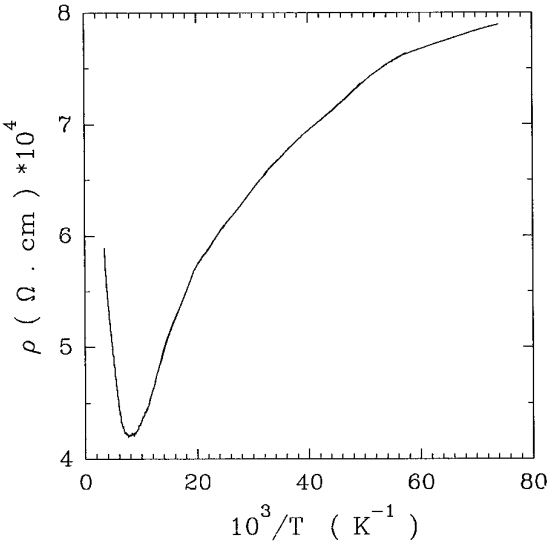

FIG. 12. Evolution of the resistivity vs $10^3/T$ of $La_{0.5}Ba_{0.5}CoO_{2.95}$.

close to 150 K. In the range $10 \leq T \leq 293$ K, the resistivity of this compound has weak values and its evolution vs temperature evidences a transition from a semi-conducting behavior below the Curie temperature to a metallic one as the temperature increases (Fig. 12). This behavior is curiously opposed to that observed for the magnetoresistive manganates $La_{1-x}A_xMnO_3$ (21) that exhibit metallic properties in the ferromagnetic state and a transition into a semi-conductor as the temperature increases near T_c. Further investigations will be needed to understand this phenomenon.

The ferromagnetism observed for $x \leq 0.25$ can be explained on the basis of the results obtained by Itoh *et al.* (9) for $La_{0.5}Sr_{0.5}CoO_3$. These authors have indeed shown that in the latter phase there exist two competing interactions that are ferromagnetic between Co(III)/Co(IV) and antiferromagnetic between Co(III)/Co(III) or Co(IV)/Co(IV). In the case of the phases $La_{0.5}Ba_{0.5}Co_{1-x}Fe_xO_{3-\delta}$, the ratio Co(III)/Co(IV) increases dramatically as x decreases (Table 4) so that the ferromagnetic coupling Co(III)–Co(IV) becomes predominant with respect to the antiferromagnetic coupling due to the pairs Co(III)–Co(III) or Co(IV)–Co(IV). However this argument does not take into account the presence of iron, the role of which cannot be neglected, although the iron content is much smaller than that of cobalt in the $x \leq 0.25$ ferromagnetic compounds.

For the iron rich phases ($x \geq 0.50$) two transition temperatures noted T_B and T_N are observed (Fig. 9). Both temperatures increase regularly with the iron content (Table 5). The above room temperature Mössbauer results allow us to confirm that T_N corresponds to the Néel transition in those antiferromagnetic phases. Whereas for T_B, at present, we cannot bring forward the origin of this transition.

TABLE 5
Magnetic Transition Temperatures Observed for the $La_{0.5}Ba_{0.5}Co_{1-x}Fe_xO_{3-\delta}$ Compounds

Composition	$T_B \pm 5$ (K)	$T_N \pm 5$ (K)
$x = 0.5$	48	142
$x = 0.75$	71	169
$x = 1$	105	218

For the $La_{0.5}Ba_{0.5}Co_{0.5}Fe_{0.5}O_{2.65}$ tetragonal phase, the temperature dependence of χ_M^{-1} is shown in Fig. 13. It shows two transitions T_B and T_N at 327 ± 5 and 480 ± 5 K, respectively. Note that T_B and T_N of this tetragonal compound are displaced to higher temperatures with respect to the oxygen rich phase $La_{0.5}Ba_{0.5}Co_{0.5}Fe_{0.5}O_{2.95}$. The detailed chemical formula proposed in the Mössbauer study shows that the main difference between the two $O_{2.65}$ and $O_{2.95}$ compositions consists, at the same time, in the disappearance of Co(IV) and the formation of Co(II) species in the reduced $O_{2.65}$ sample, while the Fe(III) content remains nearly constant.

This comparison suggests that the variation of T_B and T_N is essentially due to the change of magnetic interactions between cobalt species. The presence of the Co(II)–Co(III) couple can be brought nearer to that observed for the 112-type phase $Y_{0.5}Ba_{0.5}Co_{1-x}Cu_xO_{2.5}$ (19) for which a similar thermal evolution of χ_M^{-1} was observed with rather close values of T_B and T_N of 310 and 450 K, respectively. In the latter work, neutron diffraction studies have revealed that T_B corresponds to the change of spin orientation of the metal transition species in the structure. It seems

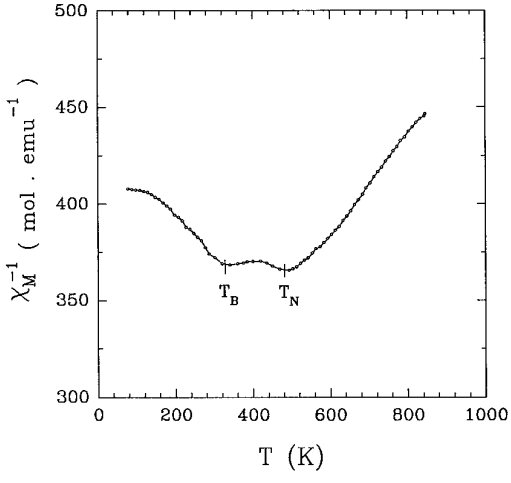

FIG. 13. Reciprocal molar magnetic susceptibility vs temperature of the $La_{0.5}Ba_{0.5}Co_{0.5}Fe_{0.5}O_{2.65}$ tetragonal compound.

probable that the T_B temperature of $La_{0.5}Ba_{0.5}Co_{0.5}Fe_{0.5}O_{2.65}$ is also related to a similar behavior.

Neutron diffraction studies will be carried out in order to explain the origin of T_B in our cubic and tetragonal phases, and eventually to determine the electronic configurations of different transition elements.

REFERENCES

1. T. C. Gibb and M. Matsuo, *J. Solid State Chem.* **81,** 83 (1989).
2. P. D. Battle, "National Institute of Standards and Technology Special Publication 804, Proceedings of the International Conference held in Jackson, WY, August 17–22, 1990." Natl. Institute of Standards and Technology, Washington, DC, 1990.
3. J. Li and J. Jing, *J. Mater. Sci.* **27,** 4361 (1992).
4. S. E. Dann, D. B. Currie, M. T. Weller, M. F. Thomas, and A. D. Al. Rawwas, *J. Solid State Chem.* **109,** 134 (1994).
5. L. Er-Rakho, C. Michel, F. Studer, and B. Raveau, *J. Phys. Chem. Solids* **48,** 377 (1987).
6. G. H. Jonker and J. H. Vansanten, *Physica* **19,** 120 (1953).
7. A. Chainani, M. Mathew, and D. D. Sarma, *Phys. Rev. B* **46,** 9976 (1992).
8. M. Abbate, J. C. Fuggle, A. Fujimori, L. H. Tjeng, C. T. Chen, R. Potze, G. A. Sawatzky, H. Elsaki, and S. Uchida, *Phys. Rev. B* **47,** 16124 (1993).
9. M. Itoh, I. Natori, S. Kuboda, and K. Motoya, *J. Phys. Soc. Jpn.* **63** (4), 1486 (1994).
10. A. Taguchi, M. Shimada, and M. Koizumi, *J. Solid State Chem.* **40,** 42 (1981).
11. Visser, J. Technisch Physische Dienst, Delft, Netherlands, ICDD Grant in Aid.
12. Y. Zhao, H. K. Liu, G. Yang, and S. X. Dou, *Physica C* **185,** 605 (1991).
13. D. B. Wiles and R. A. Young, *J. Appl. Crystallogr.* **14,** 149 (1981).
14. J. Teillet and F. Varret, unpublished MOSFIT program.
15. M. Hervieu, B. Domengès, F. Deslandes, C. Michel, and B. Raveau, *C. R. Acad. Sci. Ser. 2* **307,** 1441 (1988).
16. L. Barbey, N. Nguyen, V. Caignaert, M. Hervieu, and B. Raveau, *Mater. Res. Bull.* **27,** 295 (1992).
17. L. Errakho, C. Michel, P. Lacorre, and B. Raveau, *J. Solid State Chem.* **73,** 531 (1988).
18. V. Caignaert, I. Mirabeau, F. Bourrée, N. Nguyen, A. Ducouret, J. M. Grenèche, and B. Raveau, *J. Solid State Chem.* **114,** 24 (1995).
19. L. Barbey, N. Nguyen, V. Caignaert, F. Studer, and B. Raveau, *J. Solid State Chem.* **112,** 148 (1994).
20. F. Hartmann-Boutron, C. Meyer, Y. Gros, P. Strobel, and J. L. Tholence, *Hyperfine Interact.* **55,** 1293 (1990).
21. R. Mahesh, R. Mahendiran, A. K. Raychaudhury, and C. N. R. Rao, *J. Solid State Chem.* **114,** 297 (1995).